Deckers *et al.*: Supporting Information

S1: Polythiophene synthesis and calculation of the molar mass

The P3HTs were prepared by a Ni(dppp) - mediated (dppp = 1,3-bisdiphenylphosphino propane) polymerization using Ni(dppp)Cl_2 as an initiator and 2-bromo-5-chloromagnesio-3-hexylthiophene as monomer, which was prepared in situ from 2-bromo-5-iodo-3-hexylthiophene. This results in regioregular, head-to-tail coupled P3HTs with one -H and one -Br endgroup.[1,2] The controlled nature of the polymerization results in small polydispersities (~1.2) (See Table 1), as measured with gel permeation chromatography, and the ability to tune the degree of polymerization by adjusting monomer to initiator ratio. The gel permeation chromatography measurements were done with a Shimadzu 10A apparatus with a tunable absorbance detector in THF as eluent toward polystyrene standards.

Table 1. Molar mass, polydispersity and degree of polymerization of the P3HTs.

P3HT	Mn[a] (kg/mol)	D[a]	DP[b]
P3HT-1	1,3	1,4	5
P3HT-2	1,6	1,3	7
P3HT-3	1,9	1,2	9
P3HT-4	2,6	1,3	11
P3HT-5	3,6	1,2	14
P3HT-6	4,5	1,2	17
P3HT-7	11,0	1,2	30
P3HT-8	18,1	1,2	44
P3HT-9	36,7	1,4	100

[a] determined by GPC

[b] determined by ^{1}H NMR end-group quantification

The degree of polymerization was determined by ^{1}H NMR by end-group quantification (see Figure 1). Indeed, the α-methylenes of the 2 end-groups resonate at 2.5-2.65 ppm, while the inner α-methylenes appear at 2.65-2.9 ppm.[3] Hence, by setting the integration of the outer α-methylenes at 2, the number of inner α-methylenes is measured and the degree of polymerization can be calculated.

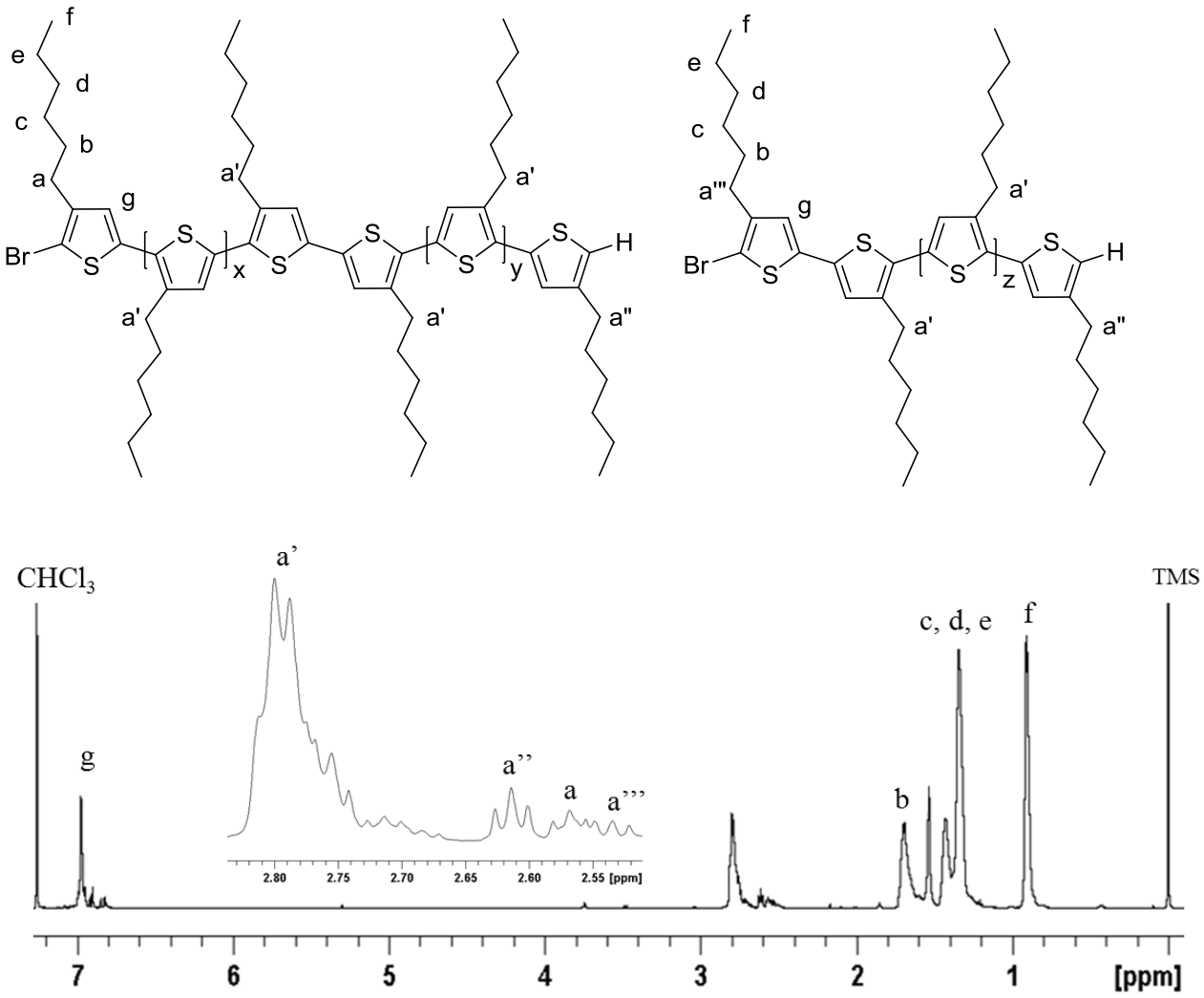

Figure 1. Assignment of the ^{1}H NMR spectrum, exemplified for **P3HT-6**.

NMR spectra of the polymers in $CDCl_3$.

a) P3HT-1

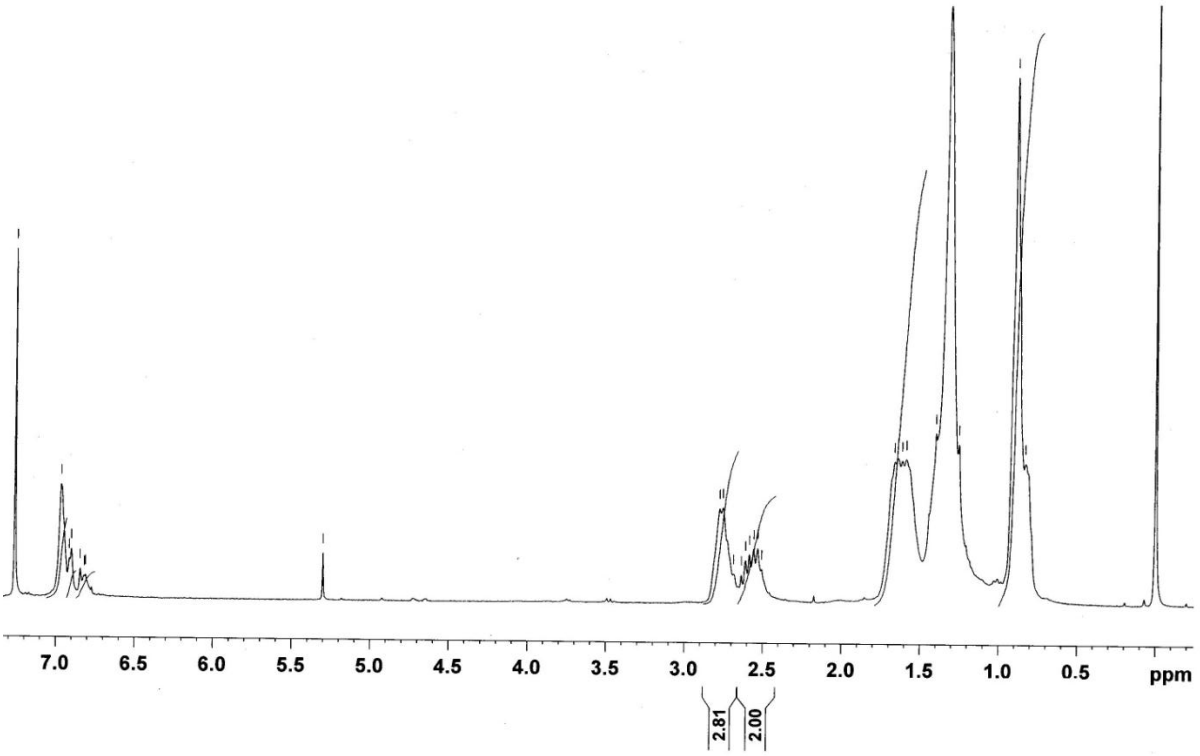

b) P3HT-2

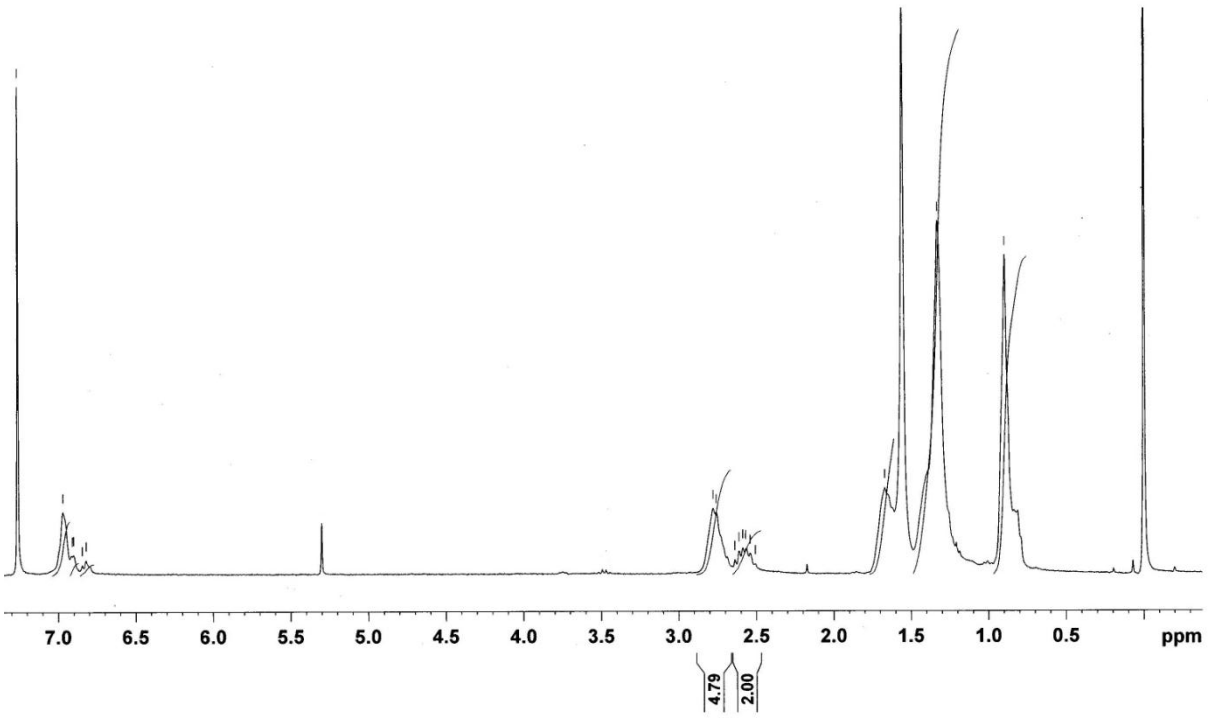

Figure 2. ^{1}H NMR spectra of the P3HT a) with 5 monomer units b) with 7 monomer units.

a) P3HT-3

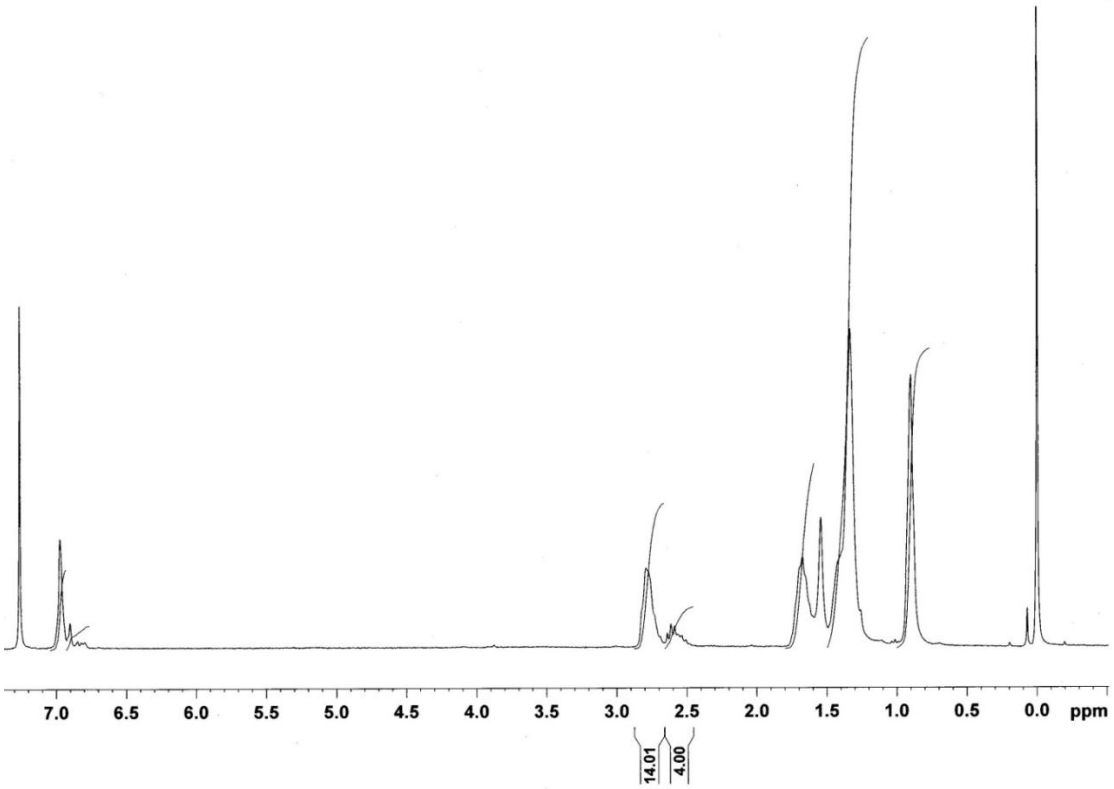

b) P3HT-4

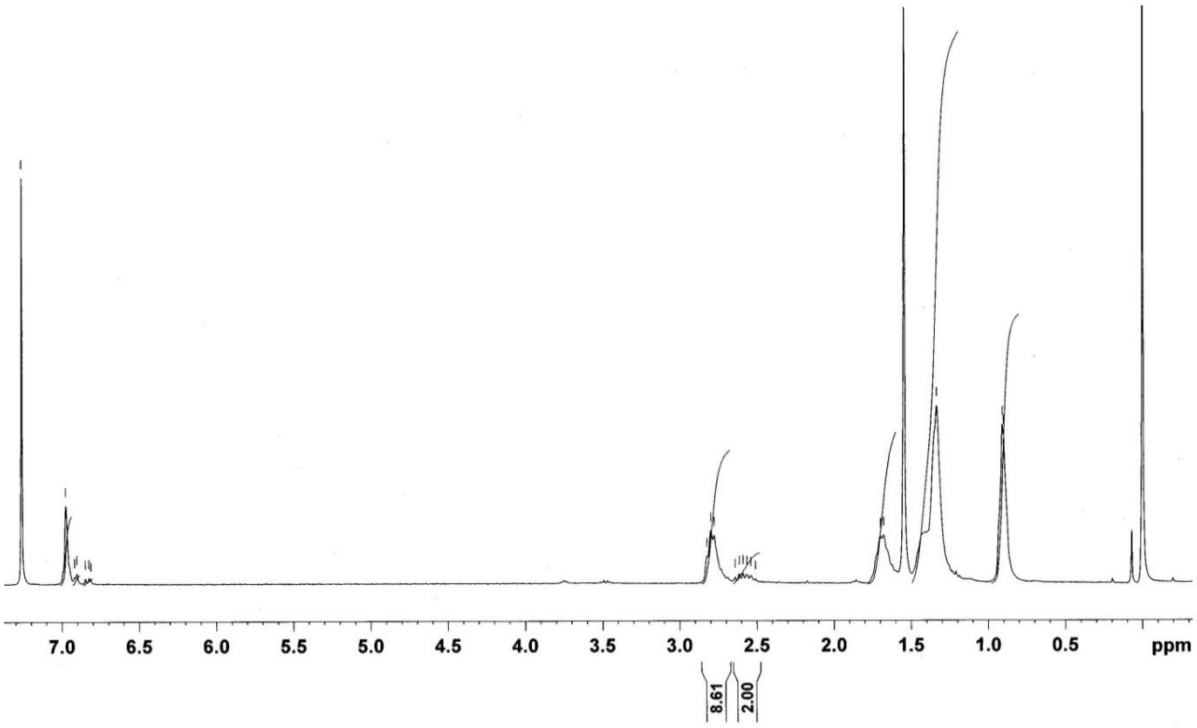

Figure 3. ^{1}H NMR spectra of the P3HT a) with 9 monomer units b) with 11 monomer units.

a) P3HT-5

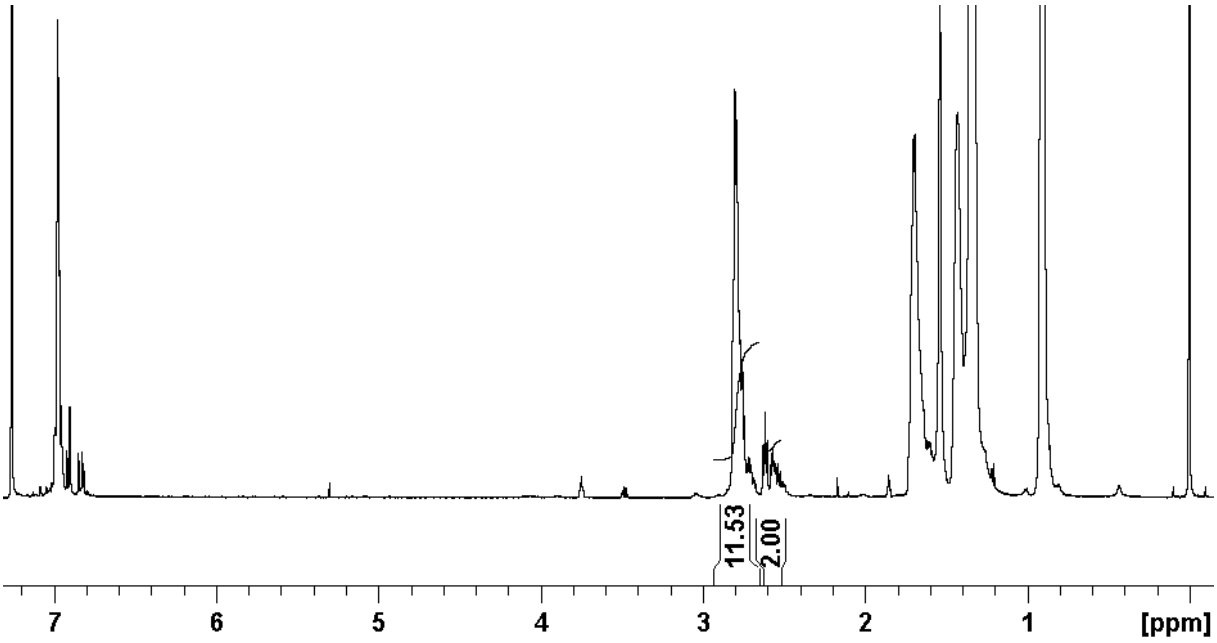

b) P3HT-6

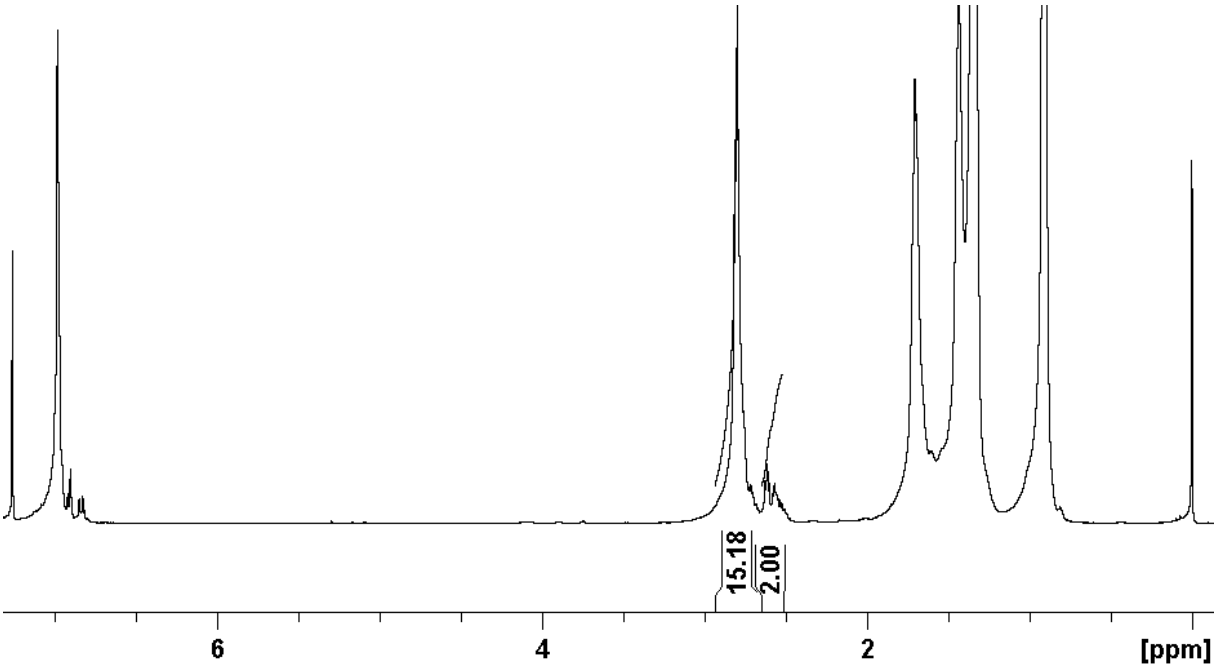

Figure 4. ^{1}H NMR spectra of the P3HT a) with 14 monomer units b) with 17 monomer units.

a) P3HT-7

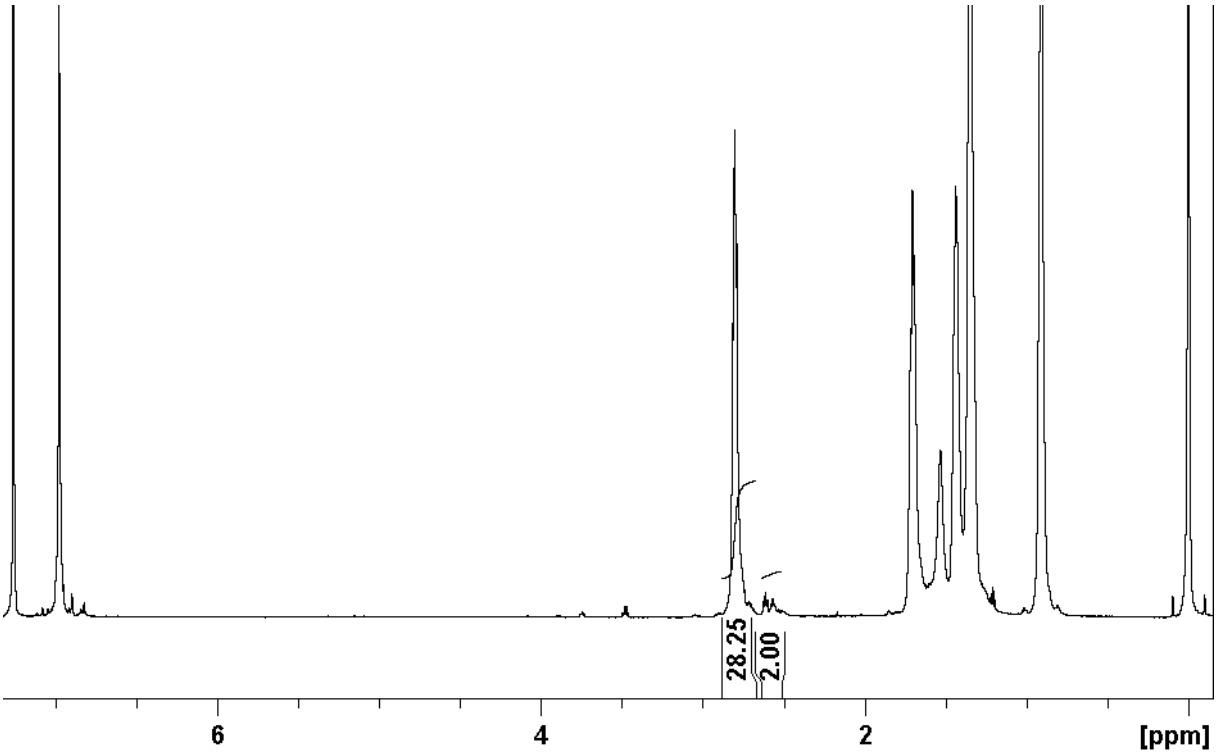

b) P3HT-8

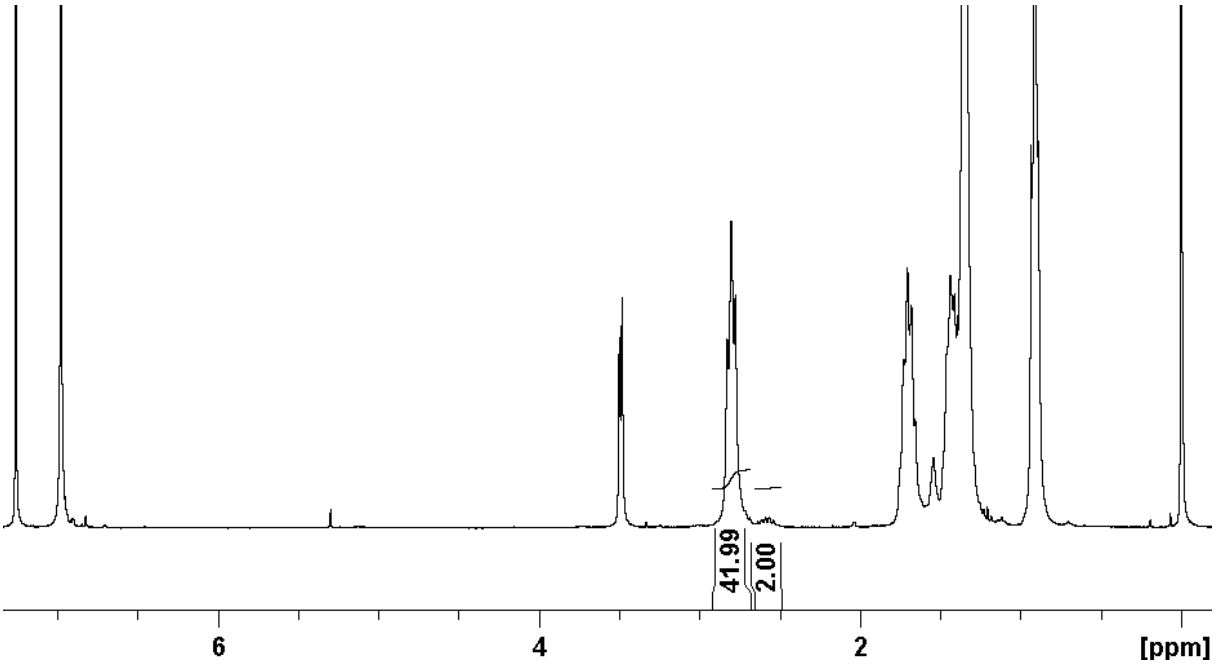

Figure 5. ^{1}H NMR spectra of the P3HT a) with 30 monomer units b) with 44 monomer units.

P3HT-9

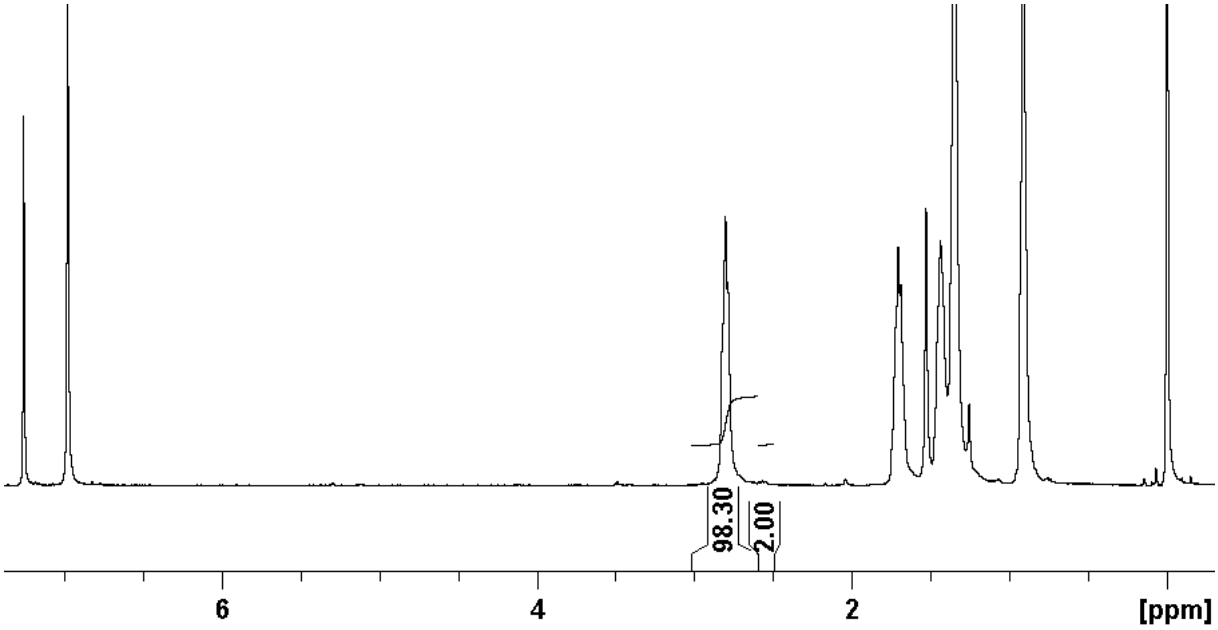

Figure 6. ^{1}H NMR spectrum of the P3HT with 100 monomer units.

Polymer synthesis: A typical polymerization procedure is as follows: The precursor monomer 2-bromo-5-iodo-3-hexylthiophene (1.00 mmol) was dissolved in dry THF (7 mL) and purged with argon. *i*-PrMgCl.LiCl (1.22 M in THF; 1.00 mmol, 0.821 mL) was added to the solution and the reaction was stirred during 45 min at room temperature. The conversion of the GRIM-reaction was evaluated by pouring an aliquot in D_2O and analyzing it with ^{1}H NMR spectroscopy. After complete conversion, the reaction mixture was added to a suspension of Ni(dppp)Cl_2 (amount determined by the monomer to initiator ratio) in dry THF (1 mL) under argon atmosphere. After 1 hour, the reaction mixture was quenched with a 2 M HCl-solution, and the polymer was precipitated in methanol, filtered off and dried under vacuum. The final polymer was a dark red-brown solid.

S2: Polythiophene (P3HTs) characterization methods

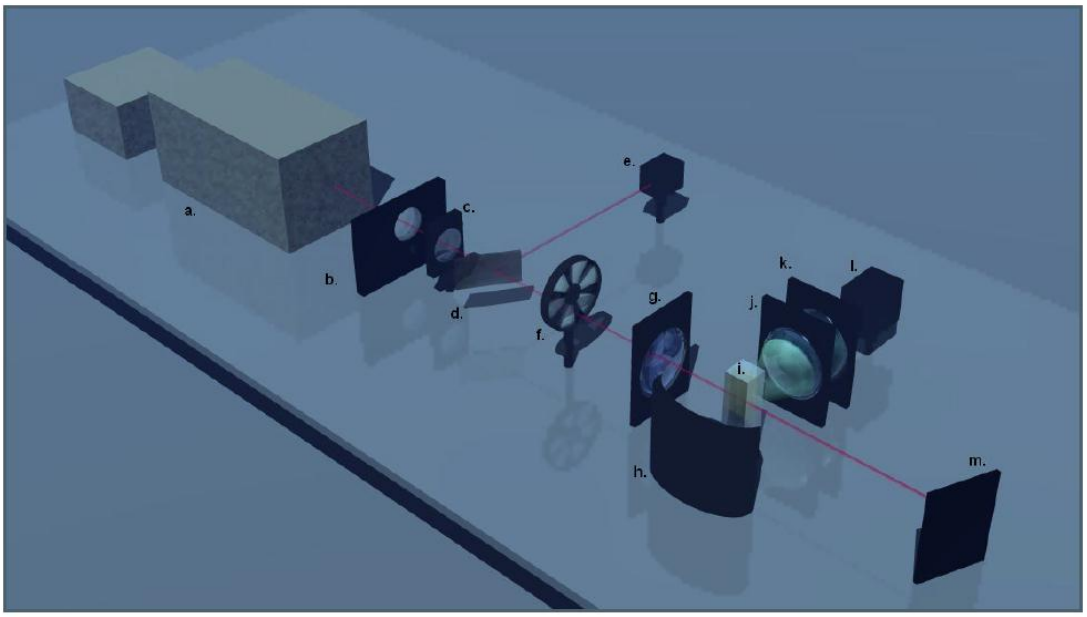

Figure 7. A 800 nm Hyper-Rayleigh Scattering set-up was used.

Nonlinear optics: The Hyper-Rayleigh Scattering (HRS) experiment was performed using a fundamental wavelength of 800 nm, originating from a Ti: sapphire laser (a, Mode-locked Tsunami 3960-LLS, Spectra Physics). At a fundamental wavelength of 800 nm this laser emits 150 fs pulses with a power of 2W and a repetition frequency of 80 MHz. The 800 nm Hyper-Rayleigh Scattering set-up is depicted in Figure 7. [4]

The vertically polarised light from the laser enters a half wave plate (CVI, model QWPM-800.0-10-2) (b) followed by a polariser (CVI, model TFPK-800.0) (c). This combination of components is used to control the intensity of the incoming laser beam of the fundamental wavelength by rotating the half wave plate and keeping the polariser fixed. The light leaving the polariser incident on the sample is vertically polarised.

A thin microscope slide (d), positioned at an angle of 45° with the fundamental laser beam, is used to divert a small fraction of the fundamental beam intensity which is analysed with a photodiode (e, Hamamatsu 2381). In case no demodulation is used, a chopper rotating with a frequency of 770 Hz (f) is added behind the polariser to modulate the beam according to the classical femtosecond HRS set-up.[5]

In case the demodulation technique is used, the chopper is omitted and a high frequency generator (Rohde & Schwarz SMG) provides the needed measurement frequency which is 770 Hz above one of the harmonics of the repetition frequency of the laser. The use of the lock-in amplifier (LIA, Stanford systems, model RS830) now permits phase-sensitive detection of the second harmonic wavelength and demodulation of the multi-photon fluorescence contribution according to Olbrechts et al.[6,7]

The sample cell is situated between a first focusing lens (focal length 100 mm) (g), a concave mirror (h), a beamstopper (m) and a collimating aspheric lens (j). The Second-Harmonic light is collected through the collimating lens (j) and focussed on the detector (l) by the focusing lens (k). Inside the detector a 10 nm interference bandpass filter (CVI, F10-400-4-1.00) ensures that only 400 nm light reaches the photomultiplier tube (Hamamatsu 6660). The detector, concave mirror, collimating lens

and the second plano convex focusing lens are situated perpendicular to the direction of the fundamental beam.

During the HRS measurements, the external reference method [8] was used with a solution of Crystal violet in methanol (Acros, HPLC grade).

UV-Vis spectroscopy and sample preparation: A Perkin-Elmer, lambda 900 spectrometer and special optical glass cuvettes with a path length of 2 mm (width 10 mm) were used. All the studied P3HTs have their main charge transfer band situated near the wavelength of the Second-Harmonic wavelength. For each P3HT sample, a dilution series in chloroform (Acros, HPLC grade) with relative concentrations 1, 4/5, 3/5, 2/5, 1/5 and 0 was created. In these dilution series, the highest concentration of P3HT was about 1.10^{-4} M ensuring that the absorbance at 400 nm does not exceed 0.1 for a path length of 2 mm. As a general rule for HRS measurements the absorbance at the Second-Harmonic wavelength should not exceed 0.1 to prevent absorption of this wavelength by the sample itself, thus interfering with the HRS measurement. Neglecting this fact causes the measured quadratic dependence of the HRS signal (to the intensity of the fundamental beam) to change considerably.

Additionally, after each HRS measurement, UV-Vis spectroscopy was used to check the P3HTs for photo-oxidation.

Normalized UV-Vis spectra: A comparison of normalized UV-Vis spectra of the studied P3HTs (see Figure 8). A clear shift of the absorbance maxima to the red part of the spectrum is visible upon adding monomer units in the polymer chain. The number of monomers is shown in the table.

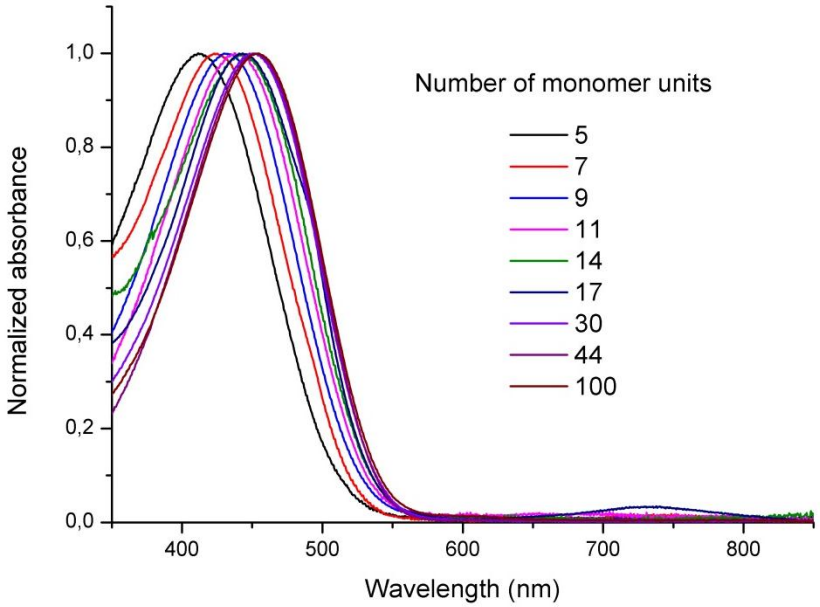

Figure 8. Comparison of normalized UV-Vis spectra of the studied P3HTs. A clear shift of the absorbance maxima to the red part of the spectrum is visible upon adding monomer units in the conjugated chain. The number of monomers is shown in the table.

For the sample consisting of 17 monomer units, a small peak was present for a few but not all of the dilutions of the concentration series. The absorbance also didn`t scale with concentration, and is thus due to an impurity. As the hyperpolarizability of this polymer follows the trend, the data were retained. The molar extinction coefficient of the small peak at 738 nm is 288 $Lmol^{-1}cm^{-1}$. The molar extinction coefficient of the main peak of this polymer is 7913 $Lmol^{-1}cm^{-1}$.

S3: Homogeneously damped Two-Level model

To calculate the static or frequency independent first hyperpolarizability β_0 we use the homogeneously broadened Two-Level model.[9] This model takes into account the width of the charge transfer band by a damping parameter γ as proposed by Orr and Ward.[10] For incoherent Hyper-Rayleigh Scattering the equation for the hyperpolarizability using the homogeneously damped Two-Level model becomes

$$\beta = \beta_0 \left\| \frac{{\omega_{eg}}^2}{3} \left[\frac{1}{(\omega_{eg} + i\gamma + 2\omega)(\omega_{eg} + i\gamma + \omega)} + \frac{1}{(\omega_{eg} - i\gamma - 2\omega)(\omega_{eg} - i\gamma - \omega)} + \frac{1}{(\omega_{eg} + i\gamma + \omega)(\omega_{eg} - i\gamma - \omega)} \right] \right\|^2$$

With β_0 the static (or frequency independent) first hyperpolarizability. The damping parameter γ equals the half-width-at-half-maximum of the long wavelength part of the absorbance peak. ω_{eg} represents the frequency of the electronic transition and ω the fundamental frequency.

S4: Calculation of transition dipole moment from UV-Vis data

For each P3HT sample, the molar extinction coefficient was plotted against the bandgap (eV). The area from the long wavelength part of these spectra was determined for each sample. Together with the energy difference of the ground state with the excited state (E) and a factor this renders the (dressed) transition dipole moment according to

$$\mu_{ge}^2 = \frac{9.13 \cdot 10^{-3}}{E} \cdot 2 \cdot area_{LWP} = \frac{9.13 \cdot 10^{-3}}{E} \cdot 2 \cdot \int \varepsilon(E) dE$$

With μ_{ge}^2 the (dressed) of the transition dipole moment between the ground state and the excited state, E the photon energy (in eV), ε the molar extinction coefficient and $area_{LWP}$ the area of the long wavelength part of the spectra.[11]

1. M. C. Iovu, E. E. Sheina, R. R. Gil, and R. D. Mccullough, *Macromolecules*, 2005, **38**, 8649–8656.

2. R. Miyakoshi, A. Yokoyama, and T. Yokozawa, *J. Am. Chem. Soc.*, 2005, **127**, 17542–7.

3. M. Verswyvel, F. Monnaie, and G. Koeckelberghs, *Macromolecules*, 2011, **44**, 9489–9498.

4. G. Olbrechts, R. Strobbe, K. Clays, and A. Persoons, *Rev. Sci. Instrum.*, 1998, **69**, 2233.

5. K. Clays and A. Persoons, *Rev. Sci. Instrum.*, 1994, **65**, 2190.

6. G. Olbrechts and R. Strobbe, *Rev. Sci. …*, 1998, **69**, 2233–2241.

7. K. Wostyn, K. Binnemans, K. Clays, and A. Persoons, *Rev. Sci. Instrum.*, 2001, **72**, 3215.

8. K. Clays, E. Hendrickx, M. Triest, and A. Persoons, *J. Mol. Liq.*, 1995, **67**, 133–155.

9. J. Campo, W. Wenseleers, E. Goovaerts, M. Szablewski, and G. H. Cross, *J. Phys. Chem. C*, 2008, **112**, 287–296.

10. B. J. Orr and J. F. Ward, *Mol. Phys.*, 1971, **20**, 513.

11. J. Pérez-Moreno, Y. Zhao, K. Clays, M. G. Kuzyk, Y. Shen, L. Qiu, J. Hao, and K. Guo, *J. Am. Chem. Soc.*, 2009, **131**, 5084–93.